Technical University of Denmark

DTU

Short-range Ferromagnetism in Alloy Ribbons of Fe-Cr-Si-Nb-(Ag, Cu)

Thanh, P. Q.; Hoa, N. Q.; Chau, N.; Huu, C. X.; Ngo, Duc-The; Phan, T. L.

DTU Library
Technical Information Center of Denmark

Short-range Ferromagnetism in Alloy Ribbons of Fe-Cr-Si-Nb-(Ag, Cu)

P. Q. THANH, N. Q. HOA and N. CHAU

Faculty of Physics, Hanoi University of Science, Vietnam National University, Hanoi, Vietnam

C. X. HUU

*Department of Electronics and Communication Engineering,
Danang University of Technology, Danang, Vietnam*

D.-T. NGO

*Department of Micro- and Nanotechnology, and Department of Energy and Storage,
Technical University of Denmark, Kgs. Lyngby 2800, Denmark*

T. L. PHAN*

Department of Physics, Chungbuk National University, Cheongju 361-763, Korea

We have studied the magnetic properties of two amorphous alloy ribbons $Fe_{72}Cr_6Si_4Nb_5B_{12}Ag_1$ (FCSNB-Ag) and $Fe_{72}Cr_6Si_4Nb_5B_{12}Cu_1$ (FCSNB-Cu), prepared by using a melt-spinning technique. Magnetization (M) measurements for various temperatures (T) and magnetic fields (H) indicate that ferromagnetic-paramagnetic (FM-PM) phase transitions take place in FCSNB-Ag and FCSNB-Cu at Curie temperatures (T_C) of about 308.3 K and 322.5 K, respectively. Analyses of $M - H$ data at different temperatures in the vicinity of the FM-PM phase transition based on the modified Arrott plot method and scaling hypothesis yielded the exponent values of $\beta = 0.369 \pm 0.005$, $\gamma = 1.359 \pm 0.005$ and $\delta = 4.7 \pm 0.1$ for FCSNB-Ag, and $\beta = 0.376 \pm 0.002$, $\gamma = 1.315 \pm 0.006$ and $\delta = 4.5 \pm 0.1$ for FCSNB-Cu. Compared with the values from theoretical models, these values are close to those expected for the 3D Heisenberg model, demonstrating the existence of short-range FM order in the amorphous alloy ribbons.

I. INTRODUCTION

Currently, Fe-, Ni- and Co-based amorphous alloys are still an issue of intensive interest because of their promising applications in devices for conversion of electromagnetic energy into mechanic energy, magnetic refrigerator, sensitive sensors, telecommunications, automotive magnetics, and electronic article surveillance [1–4]. Compared with the conventional alloys NiFe, FeCo and FeSi, these amorphous alloys exhibit some rotable properties, such as high corrosion resistance, relatively great saturation magnetization, and soft-magnetic behavior (*i.e.*, small coercivity, leading to low hysteretic losses). Depending on the applications, these properties can be easily modified by changing the dimension and compositions of the amorphous alloys. These amorphous alloys are a promising new class of materials where applications are in competition with those of the conventional alloys. Particularly, the addition of Ti, Cr, Nb, Si, B and/or Cu to Fe- and Co-metalloid alloys remarkably improves their corrosion resistance and soft-magnetic behaviors [2, 5–7]. Here, the combination of chemical elements with different atomic radii stimulates structural disorder (short-range structure) so that the amorphous phase can be easily formed and ferromagnetic-paramagnetic (FM-PM) phase-transition temperature (the Curie temperature, T_C) can be controlled.

Recently, more and more attention has focused on fabricating and studying amorphous alloy ribbons for magnetic-refrigeration technology, which is based on the magnetocaloric (MC) effect [2, 3, 8–10]. This effect is directly related to the temperature change (or magnetic-entropy change) under adiabatic conditions of a ferromagnet under an external applied field. The temperature (or magnetic-entropy) change is strongest around the FM-PM phase-transition temperature T_C, where

*E-mail: ptlong2512@yahoo.com; Fax: +82-43-275-6416

magnetic moments become disordered due to the thermal activation energy [11]. For conventional applications in cooling systems (such as air conditioners, refrigeration and freezers), the T_C of amorphous alloys can be controlled in the temperature range of 260 ∼ 310 K. For example, the T_C values of the amorphous alloy ribbons $Fe_{78}Nb_5Si_4B_{12}Cu_1$ (> 450 K) [8, 9] and $Fe_{73.5}Nb_3Si_{13.5}B_9Au_1$ (> 600 K) [12] can be reduced to lower temperatures by doping Cr into the Fe site. Though many works have focused on the physical properties of Cr-doped Fe-Nb-Si-B-Cu-based amorphous alloy ribbons [7–9,13], the magnetic interactions around their FM-PM phase transitions have not been intensively studied. Additionally, no work in reference to the magnetic properties of (Cr, Ag)-codoped Fe-Nb-Si-B alloy ribbons seems to exist. To get more insight into these material systems, we prepared two amorphous alloy ribbons $Fe_{72}Cr_6Si_4Nb_5B_{12}Cu_1$ and $Fe_{71}Cr_7Si_4Nb_5B_{12}Ag_1$, and then studied their magnetic properties based on magnetization (M) versus temperature (T) and magnetic field (H) measurements. Based on the mean-field theory for a second-order magnetic phase transition (SOMT) associated with long-range magnetic interactions [14], we determined the values of the critical exponents β, γ and δ associated with the temperature dependences of the saturation magnetization, $M_s(T)$, the inverse initial susceptibility, $\chi_0^{-1}(T)$, and the critical isotherm M, respectively. Compared with the theoretical values, these experimentally-determined values are close to those expected for the 3D Heisenberg model [15], demonstrating the existence of short-range FM order in the amorphous alloy ribbons.

II. EXPERIMENTAL DETAILS

Two amorphous ribbons (the widths and thicknesses are of about 2-6 mm and 20 μm, respectively) with nominal compositions of $Fe_{71}Cr_7Si_4Nb_5B_{12}Ag_1$ (FCSNB-Ag) and $Fe_{72}Cr_6Si_4Nb_5B_{12}Cu_1$ (FCSNB-Cu) were prepared from high-purity elements (> 3N) as precursors by using the melt-spinning technique. The fabrication was carried out in a vacuum chamber at 10^{-4} Torr, and that pressure was maintained by using an Ar gas flow. After preparation, the amorphous phase in the final ribbon products was confirmed by using X-ray diffraction [9]. Magnetization versus temperature and magnetic field measurements were performed on a vibrating sample magnetometer (VSM), where the temperature and the magnetic field could be changed from 100 to about 500 K and from 0 to 10 kOe, respectively. To study the critical behavior of the alloy ribbons, we used Arrott plots [16,17] and the scaling hypothesis [15] to analyze the $M - H - T$ data in the vicinity of the T_C.
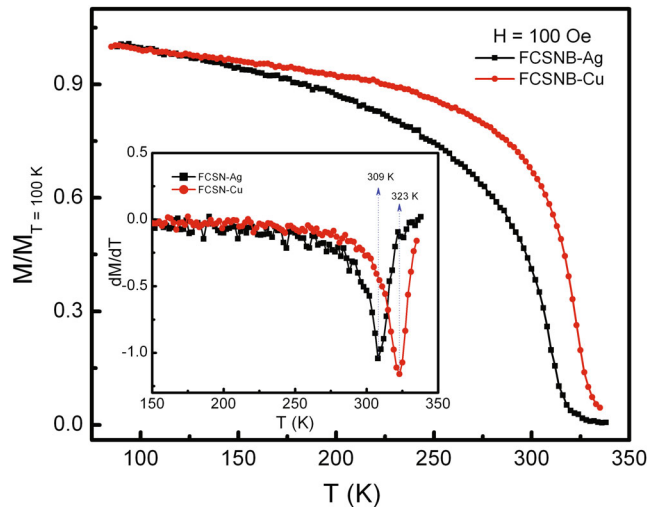

Fig. 1. (Color online) Temperature dependences of magnetization normalized to the value at 100 K, $M/M_T = 100$ K, for the amorphous alloy ribbons in the field $H = 100$ Oe. The inset shows dM/dT versus T curves.

III. RESULTS AND DISCUSSION

Figure 1 shows the temperature dependences of the zero-field-cooled magnetization normalized to the value at 100 K for the amorphous alloy ribbons FCSNB-Ag and FCSNB-Cu in the field $H = 100$ Oe. The gradual decrease in the magnetization at low temperatures can be seen to become rapid when the temperature is higher than 290 K, which is due to the FM-PM phase transition taking place at the T_C. At temperatures above the T_C, the samples are in the PM state; thus, the magnetization decreases to zero. From the dM/dT versus T curves, we obtained the T_C values (from the minima of the curves, as shown in the inset of Fig. 1) of FCSNB-Ag and FCSNB-Cu to be about 309 K and 323 K, respectively. If more attention is given to the variation of the $M(T)$ curves, that variation is quite different, particularly at temperatures above 150 K. While high M values and a narrower FM-PM transition region are observed for FCSNB-Cu, such features are absent from FCSNB-Ag. To explain the obtained results, we consider the Cr content in the alloy ribbons because both Ag and Cu in the same amounts are diamagnetic. The Cr content in FCSNB-Ag (7 at.%) appears to be higher than that in FCSNB-Cu (6 at.%). According to previous studies [8, 9], the T_C and M values of FCSNB-Ag should be smaller than those of FCSNB-Cu. However, such scenarios do not occur in the present case. This proves that the differences in the T_C and M values, and in the characteristic phase transition not only depend on Cr-doping content but also on the natures of the Ag and Cu elements present in the FCSNB host, where the Fe-related FM phase plays an important role.

To further understand the magnetic properties of FCSNB-Ag and FCSNB-Cu, we recorded magnetic-field
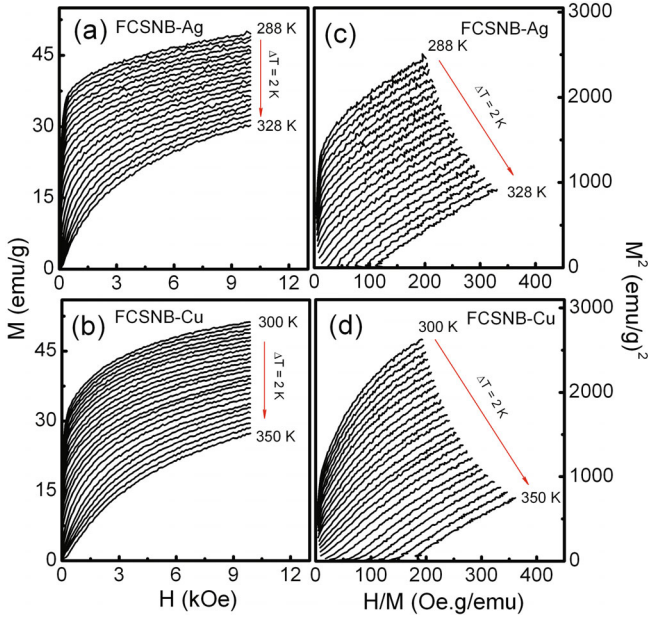
Fig. 2. (Color online) (a, b) $M(H)$ curves and (c, d) Arrott plots of M^2 versus H/M for amorphous alloy ribbons of FCSNB-Ag and FCSNB-Cu at temperatures around the FM-PM phase transitions.

dependences of the initial magnetization, $M(H)$, at different temperatures and then studied their critical behavior by determining the values of the exponents β, γ and δ. As shown in Figs. 2(a) and (b), the magnetization gradually decreases, and the nonlinear $M(H)$ curves in the FM region tend to become linear with increasing temperature because the samples go into the PM state. Though the field is increased up to 10 kOe, no saturation magnetization occurs. This phenomenon was also observed in $Fe_{70}Cr_8Si_4Nb_5B_{12}Cu_1$ [8] and in other alloy ribbons [4,18], which is a characteristic of ferromagnets without true long-range magnetic order. According to the mean-field theory (MFT) proposed for a ferromagnet exhibiting a SOMT and long-range magnetic interactions [14], the free energy G_L can be expanded in even powers of M as follows:

$$G_L = aM^2 + bM^4 + \ldots - HM, \qquad (1)$$

where a and b are temperature-dependent parameters. Minimizing G_L gives the relation:

$$H/M = 2a + 4bM^2. \qquad (2)$$

This equation indicates that when the magnetic interactions in a ferromagnet obey the MFT, the plots of M^2 versus H/M around the T_C are parallel straight lines. Particularly, the M^2 versus H/M line at the T_C passes through the coordinate origin, as in Arrott plots [16,17]. However, these features are not observed in Figs. 2(c) and (d), which means that magnetic interactions in our amorphous alloys FCSNB-Ag and FCSNB-Cu do not
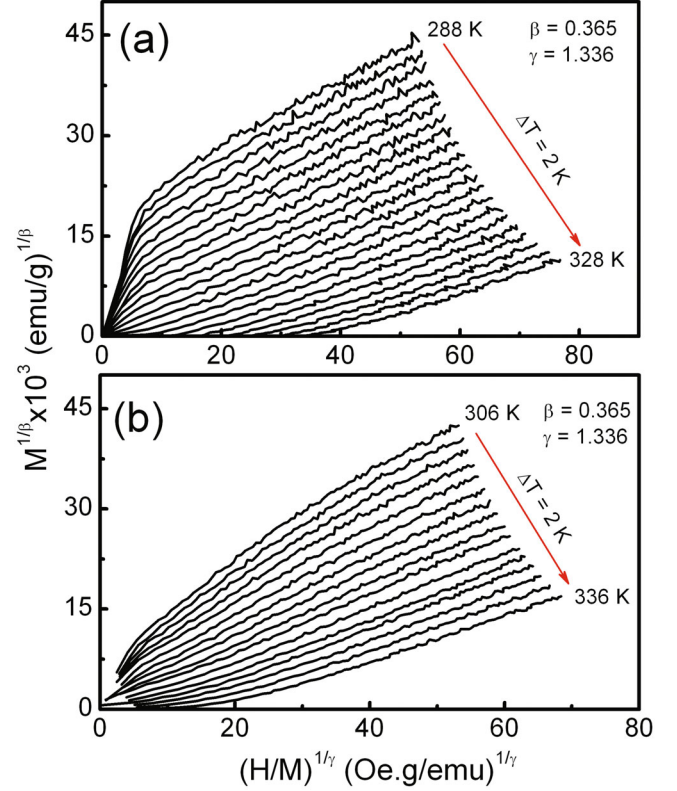

Fig. 3. (Color online) Modified Arrott plots with trial exponents $\beta = 0.365$ and $\gamma = 1.336$ expected for the 3D Heisenberg model.

have long-range order. More evidence supporting this conclusion can be gotten from the critical exponents β, γ and δ. Within the framework of the MFT, Eq. (2) for modified Arrott plots (MAP) can be generalized by using the scaling equation of state [17]

$$(H/M)^{1/\gamma} = c_1 \varepsilon + c_2 M^{1/\beta}, \qquad (3)$$

where c_1 and c_2 are temperature-dependent parameters, and $\varepsilon = (T - T_C)/T_C$ is the reduced temperature. In this equation, the β, γ and δ values can be obtained from the asymptotic relations

$$M_s(T) = M_0(-\varepsilon)^\beta, \qquad \varepsilon < 0, \qquad (4)$$
$$\chi_0^{-1}(T) = (h_0/M_0)\varepsilon^\gamma, \qquad \varepsilon > 0, \qquad (5)$$
$$M = DH^{1/\delta}, \qquad \varepsilon = 0, \qquad (6)$$

where M_0, h_0, and D are the critical amplitudes. We should notice that if $\beta = 0.5$ and $\gamma = 1.0$, Eq. (3) returns the form of Eq. (2). However, these β and γ values are not suitable for describing magnetic interactions taking place in our alloys. Thus, more accurate values are needed. In the present work, we have used the MAP method, starting from the scaling equation of state with trial exponent values of $\beta = 0.365$ and $\gamma = 1.336$ expected for the 3D Heisenberg model [15]. As mentioned above, correct β and γ values make the $M(H)$ data falling on a
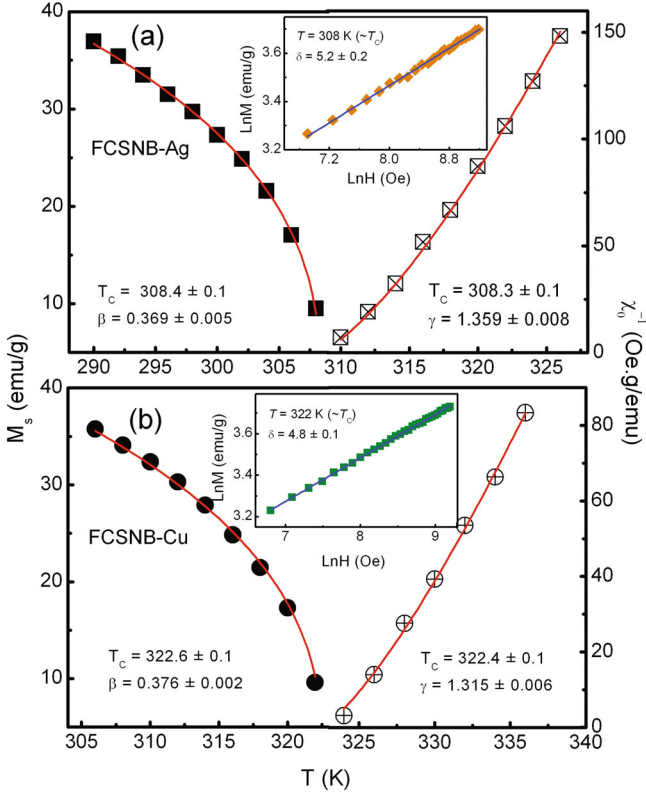
Fig. 4. (Color online) $M_s(T)$ and $\chi_0^{-1}(T)$ data around T_C fitted to Eqs. (4) and (5), respectively, for (a) FCSNB-Ag and (b) FCSNB-Cu. The insets show the isotherms at temperatures close to T_C fitted to Eq. (6).

Fig. 5. (Color online) Scaling performance of $M/|\varepsilon|^{\beta}$ versus $H/|\varepsilon|^{\beta+\gamma}$ for the $M-H-T$ data around the T_C values of two alloy ribbons: (a) FCSNB-Ag and (b) FCSNB-Cu.

set of parallel straight lines in the performance of $M^{1/\beta}$ versus $(H/M)^{1/\gamma}$, and the $M^{1/\beta}$ versus $(H/M)^{1/\gamma}$ lines pass through the origin at the T_C. These features can be clearly seen in Fig. 3 for magnetic fields $H > 3$ kOe, proving that the values of the critical exponents associated with short-range magnetic interactions of the 3D Heisenberg and/or 3D Ising models are more suitable for describing our system.

With the trial exponent values and the MAP shown in Fig. 3, $M_s(T)$ and $\chi_0(T)$ data obtained from the linear extrapolation in the high-field region ($H > 3$ kOe) to the $M^{1/\beta}$ and $(1/\chi_0)^{1/\gamma}$ axes are then fitted to Eqs. (4) and (5), respectively, to achieve better β, γ and T_C values. These new values of β, γ and T_C are continuously used for the next MAP processes until their optimal values are achieved. Notably, during the best fitting process, the T_C values determined from the $M(T)$ data (shown in Fig. 1) were used as a reference. The final results are shown in Fig. 4 and Table 1, where the values of the critical parameters are $T_C \approx 308.3$ K, $\beta = 0.369 \pm 0.005$, $\gamma = 1.359 \pm 0.005$ and $\delta = 4.7 \pm 0.1$ for FCSNB-Ag and $T_C \approx 322.5$ K, $\beta = 0.376 \pm 0.002$, $\gamma = 1.315 \pm 0.006$ and $\delta = 4.5 \pm 0.1$ for FCSNB-Cu. The T_C values obtained in this case can be seen to be very close to those obtained from the $M(T)$ data.
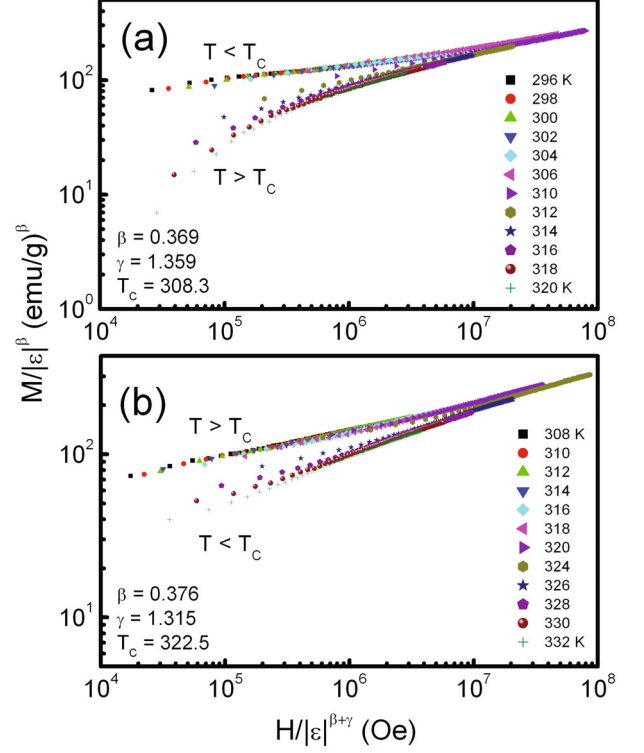
The reliability of the exponent values can be checked by means of the static-scaling hypothesis, which states that M is a function of ε and H, $M(H,\varepsilon) = |\varepsilon|^{\beta} f_{\pm}(H/|\varepsilon|^{\beta+\gamma})$, where f_+ and f_- are analytic functions for $T > T_C$ and $T < T_C$, respectively [15]. This equation implies that, with the determined β and γ values, all $M(H)$ data points fall onto two universal branches of f_- and f_+ in M/ε^{β} versus $H/\varepsilon^{\beta+\gamma}$ curves. Clearly, such descriptions are in good agreement with the features of the high-field region shown in Fig. 5, demonstrating the reliability of the β and γ values determined in our work. It should be noticed that, in the low-field region, due to rearrangement of magnetic domains and the uncertainty in the calculation of demagnetization factor, unexpected errors for critical values can thus be occurred, leading to the scattering of the $M-H$ data points from the universal curves. For the last exponent δ, its values obtained from the Widom relation of $\delta = 1 + \gamma/\beta$ [15] for FCSNB-Ag and FCSNB-Cu are 4.7 ± 0.1 and 4.5 ± 0.1, respectively, which are close to those obtained from the fitting the $M(H)$ isotherms at 308 K ($\sim T_C$) for FCSNB-Ag and 322.4 K ($\sim T_C$) for FCSNB-Cu to Eq. (5), as shown in the insets of Fig. 4.

The comparison of the theoretical and experimental values in Table 1 shows that the β, γ and δ values obtained in our work are quite close to those expected from the 3D Heisenberg model with $\beta = 0.365$, $\gamma = 1.336$ and $\delta = 4.8$. This once again proves the existence of

Table 1. Values of the critical parameters of FCSNB-Ag and FCSNB-Cu alloy ribbons compared with those of the theoretical models and of some Fe-based amorphous alloys reported previously using the MAP method. Here, δ values are mainly calculated from the Widom relation $\delta = 1 + \gamma/\beta$.

Model/Material	T_C (K)	β	γ	δ	Ref.
Mean-field theory	-	0.5	1.0	3.0	15
3D Heisenberg model	-	0.365	1.336	4.8	15
3D Ising model	-	0.325	1.241	4.82	15
$Fe_{72}Cr_6Si_4Nb_5B_{12}Ag_1$	308.3	0.369 ± 0.005	1.359 ± 0.008	4.7 ± 0.1	This work
$Fe_{72}Cr_6Si_4Nb_5B_{12}Cu_1$	322.5	0.376 ± 0.002	1.315 ± 0.006	4.5 ± 0.1	This work
$Fe_{70}Cr_8Si_4Nb_5B_{12}Cu_1$	285	0.31 ± 0.02	1.60 ± 0.02	6.2 ± 0.1	8
$Fe_{76}Cr_{2.5}B_{13.5}Si_8$	613	0.398	1.38	4.5	19
$Fe_{75.5}Cr_4B_{13}Si_{7.5}$	567	0.366	1.286	4.8	19
$Fe_{73.6}Cr_{6.5}B_{14.6}Si_{5.3}$	430	0.358	1.365	4.8	19
$Fe_{90}Zr_{10}$	227	0.345	1.395	5.0	20
$Fe_{86}Mn_4Zr_{10}$	213	0.369	1.368	4.7	20
$Fe_{84}Mn_6Zr_{10}$	197	0.341	1.358	5.0	20
$Fe_{82}Mn_8Zr_{10}$	185	0.365	1.387	4.8	20
$Fe_{80}Mn_{10}Zr_{10}$	169	0.368	1.384	4.8	20
$Fe_{78}Mn_{12}Zr_{10}$	154.3	0.359	1.378	4.8	20
$(Fe_{0.74}Cu_{0.26})_{85}Zr_{15}$	326.5	0.52	1.01	3.15	21
$Fe_{77}Co_{5.5}Ni_{5.5}Zr_7B_4Cu_1$	493	0.53 ± 0.03	1.34 ± 0.04	3.5 ± 0.4	22

short-range FM order in the amorphous alloy ribbons. Previous studies on some Fe-based amorphous alloy ribbons also revealed the same result [8, 19, 20]. Very few works have found exponent values associated with long-range FM interactions [21, 22] (see Table 1). Recently, with simple models of magnetism, Skomski has showed that long-range FM interactions could be established in complicated spin structures, including FM, anti-FM and non-collinear magnetic materials [23]. In fact, the values of the critical exponents depend strongly on the range of the exchange interaction $J(r)$, spins, and the spatial dimensionality. Using the renormalization group approach for an exchange-interaction system, Fisher and co-workers [24] found that the exponent values depended on the exchange-interaction range characterized by $J(r) = 1/r^{d+\sigma}$, where d and σ are the dimension and the interaction range, respectively, of the system. The mean-field-theory exponents are valid for $\sigma < \frac{1}{2}$ while the Heisenberg ones are valid for $\sigma > 2$. The exponents belong to other universality classes if $\frac{1}{2} < \sigma < 2$. Additionally, depending on the nature and structure of alloy ribbons (*i.e.*, amorphous and/or nanocrystals embedded in an amorphous host) [10, 21, 22], long- and short-range magnetic interactions may coexist.

IV. CONCLUSION

The magnetic and critical properties of the amorphous alloy ribbons, FCSNB-Ag and FCSNB-Cu, were studied in detail by means of $M(H,T)$ data. Experimental results revealed that FM-PM phase transitions take place in FCSNB-Ag and FCSNB-Cu at $T_C \approx 308$ K and 322 K, respectively. Using the SOMT theory, MAP method and scaling hypothesis, we determined the values of the critical exponents for the alloy ribbons, with $\beta = 0.369 - 0.376$, $\gamma = 1.315 - 1.359$ and $\delta = 4.5 - 4.7$. These values appear to be quite close to those expected for the 3D Heisenberg ($\beta = 0.365$ and $\gamma = 1.336$) and reveal the presence of short-range magnetic interactions in the amorphous alloy ribbons. Because of the different values of magnetization and critical parameters (T_C, β, γ and δ) obtained for two samples, we believe that the characteristic of the FM and PM phases in FCSNB-Ag and FCSNB-Cu depend not only on Cr-doping content but also on the physical nature of the elements Ag and Cu present in the FCSNB host.

ACKNOWLEDGMENTS

REFERENCES

[1] I. Betancourt, Materials **4**, 37 (2011).

[2] H. G. Kim, M. S. Kim and W. N. Myung, J. Korean Phys. Soc. **49**, 1630 (2206).

[3] T. D. Thanh, Y. K. Yu, P. T. Thanh, N. H. Yen, N. H. Dan, T. L. Phan, A. M. Grishin and S. C. Yu, J. Appl. Phys. **113**, 213908 (2013).

[4] T. L. Phan, P. Zhang, N. H. Dan, N. H. Yen, P. T. Thanh, T. D. Thanh, M. H. Phan and S. C. Yu, Appl. Phys. Lett. **101**, 212403 (2012).

[5] M. Naka, K. Hashimoto and T. Masumoto, J. Non-cryst. Solids **31**, 355 (1979).

[6] Y. Yoshizawa, S. Oguma and K. Yamauchi, J. Appl. Phys. **64**, 6044 (1998).

[7] T. Choh, H. Chihara, M. Igarashi, O. Kohmoto and Y. Narumiya, IEEE Translat. J. Magn. Jpn. **7**, 384 (1992).

[8] A. Kolano-Burian, M. Kowalczyk, R. Kolano, R. Szymczak, H. Szymczak and M. Polak, J. Alloys Compd. **479**, 71 (2009).

[9] C. X. Huu, N. Chau, N. D. The and N. Q. Hoa, J. Korean Phys. Soc. **53**, 763 (2008).

[10] T. D. Thanh, N. H. Yen, P. T. Thanh, N. H. Dan, P. Zhang, T. L. Phan and S. C. Yu, J. Appl. Phys. **113**, 17E123 (2013).

[11] V. Franco, J. S. Blazquez, B. Ingale and A. Conde, Annu. Rev. Mater. Res. **42**, 305 (2012).

[12] S. G. Min, L. G. Ligay, K. S. Kima, S. C. Yu, N. D. Tho and N. Chau, J. Magn. Magn. Mater. **300**, e385 (2006).

[13] C. F. Conde, M. Millan, J. M. Borrego, A. Conde, M. J. Capitan and J. L. Joulaud, Philosophical Magazine Lett. **78**, 221 (1998).

[14] J. M. D. Coey, *Magnetism and Magnetic Materials* (Cambridge University Press, Cambridge, 2010).

[15] H. E. Stanley, *Introduction to Phase Transitions and Critical Phenomena* (Oxford University Press, London, 1971).

[16] A. Arrott, Phys. Rev. **108**, 1394 (1957).

[17] A. Arrott and J. E. Noakes, Phys. Rev. Lett. **19**, 786 (1967).

[18] B. M. Wang, L. Wang, Y. Liu and B. C. Zhao, J. Appl. Phys. **105**, 023913 (2009).

[19] I. M. Kyprianidis, C. A. Achilleos, I. A. Tsoukalas, H. Bremers and J. Hesse, J. Magn. Magn. Mater. **161**, 203 (1996).

[20] A. Perumal, V. Srinivas, K. S. Kim, S. C. Yu, V. V. Rao and R. A. Dunlap, Phys. Rev. B **65**, 064428 (2002).

[21] F. J. Castano, J. M. Garcia-Beneytez, P. Crespo, M. Multigner, M. Vazquez and A. Hernando, J. Phys. Condens. Matter **11**, 5671 (1999).

[22] V. Franco, R. Caballero-Flores, A. Conde, K. E. Knipling and M. A. Willard, J. Appl. Phys. **109**, 07A905 (2011).

[23] R. Skomski, *Simple Model of Magnetism* (Oxford University Press, London, 2008).

[24] M. E. Fisher, S. K. Ma and B. G. Nickel, Phys. Rev. Lett. **29**, 917 (1972).